

## *Supporting Information:*

# **Chemical Identification of Interlayer Contaminants within van der Waals Heterostructures**

*Jeffrey J. Schwartz,<sup>†,‡</sup> Hsun-Jen Chuang,<sup>§</sup> Matthew R. Rosenberger,<sup>§</sup> Saujan V. Sivaram,<sup>§</sup>  
Kathleen M. McCreary,<sup>§</sup> Berend T. Jonker,<sup>\*,§</sup> Andrea Centrone,<sup>\*,†</sup>*

<sup>†</sup>Physical Measurement Laboratory, National Institute of Standards and Technology,  
Gaithersburg, MD 20899, United States

<sup>‡</sup>Institute for Research in Electronics and Applied Physics, University of Maryland, College  
Park, MD 20742, United States

<sup>§</sup>Materials Science & Technology Division, Naval Research Laboratory, Washington, D.C.  
20375, United States

Contact Information:

\*E-mail: [berry.jonker@nrl.navy.mil](mailto:berry.jonker@nrl.navy.mil)

\*E-mail: [andrea.centrone@nist.gov](mailto:andrea.centrone@nist.gov)

**SUPPORTING INFORMATION CONTENTS:**

**PDMS Cleaning: Mass Change**

**Van der Waals Heterostructure Fabrication Methods**

**PDMS All-Dry Transfer**

**Water-Assisted PDMS Pick-up and Transfer**

**Polymer-Assisted Dry Pick-up and Transfer**

**Molecular Structures**

**Spectral Processing**

**Image Processing**

**Reference Absorption Spectra**

**Additional PTIR Absorption Spectra**

**Nanocontaminant Quantity Estimation**

**Supplementary References**

## PDMS Stamp Cleaning: Mass Change

The mass of each polydimethylsiloxane (PDMS) stamp was measured both prior to cleaning and after drying, see Table S1. The observed mass loss as a result of the cleaning process corresponds roughly to the PDMS swelling ratios in the solvents used here.<sup>1</sup> However, the mass loss is not an effective predictor of the cleaning method effectiveness since the two solvents that reduced the amount of PDMS contaminants in van der Waals heterostructures (vdWHs), as determined by photothermal induced resonance spectra (PTIR), lie near opposite ends of this spectrum. Toluene, a relatively non-polar solvent, is absorbed readily into the oleophilic PDMS matrix, whereas isopropanol is relatively polar and results in only minor swelling of the stamp.

**Table S1.** Change in polydimethylsiloxane stamp mass after washing in designated solvent.

Solvent	Starting Mass <sup>a</sup> (mg)	Mass Loss <sup>a</sup> (mg)	Mass Loss (%)
Acetone	5.5	0.1	1.8
Toluene	7.9	0.4	5.1
Isopropanol	10.6	0.0	0.0
Hexane	9.8	0.9	9.2

<sup>a</sup>Mass measurements are limited by the precision (0.1 mg) of the digital scale used in these experiments.

## Van der Waals Heterostructure Fabrication Methods

*PDMS All-Dry Transfer<sup>2</sup> (hBN/hBN):* Flakes of hBN, carried on PDMS stamps, were aligned and then brought into contact with complementary flakes on Au-coated SiO<sub>2</sub> substrates. Afterward, peeling the PDMS stamps away from the substrates resulted in the stacked flakes adhering to the Au-coated substrate and forming a nominal hBN/hBN heterostructure. See Figure S1.

*Water-Assisted PDMS Pick-up and Transfer<sup>2-5</sup> (hBN/hBN; TMD/hBN; TMD/TMD):* Regions of SiO<sub>2</sub>/Si substrates, supporting flakes of either hBN or a TMD, were contacted by PDMS stamps. Single drops of a water-isopropanol (1:1) mixture were applied to the stamp/substrate junctions from the side, which spread quickly over the hydrophilic SiO<sub>2</sub> surfaces. Gradually lifting the PDMS stamps from the substrates drew in the water-isopropanol mixture, enabling it to wet the surfaces beneath the flakes and causing the flakes to transfer to the PDMS stamp. The stamps were then immediately blown dry with nitrogen gas. Next, the flakes were deposited onto other substrates or flakes, as described above. See Figure S2.

*Polymer-Assisted Dry Pick-up and Transfer<sup>6</sup> (hBN/hBN):* Polycarbonate-coated stamps (PC/PDMS/glass) were placed in contact with selected flakes of hBN. While in contact, the substrates were heated to 110 °C before lifting the stamps, which carried the targeted flakes with them adhered to the PC film. Next, the hBN flakes on PC/PDMS/glass stamps were set atop other flakes, supported by either Au-coated SiO<sub>2</sub>, SiO<sub>2</sub>, or Si substrates. To deposit the flakes, the substrates were heated to 135 °C, thereby releasing the PC films from the PDMS and forming a PC/flake/flake structure. Later, the substrates were cooled to 40 °C and immersed in chloroform

for 10–15 min to remove the exposed PC films. Finally, the vdWHs were rinsed with isopropanol and blown dry with nitrogen gas. See Figure S3.

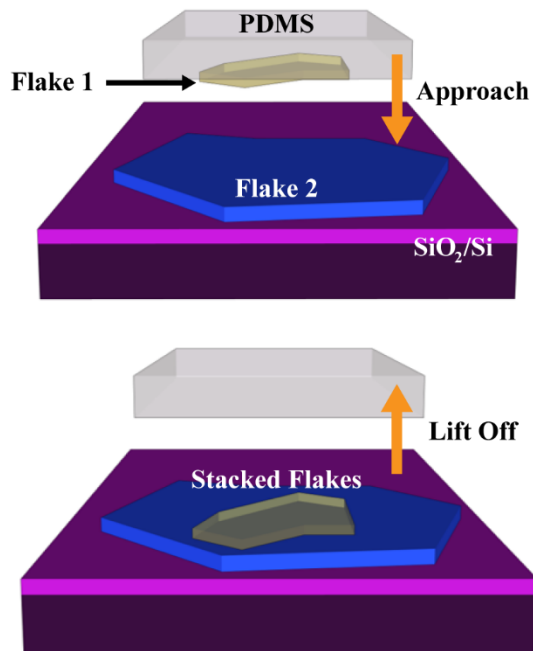


**Figure S1.** Schematic illustrating the PDMS all-dry transfer method of van der Waals heterostructure fabrication.

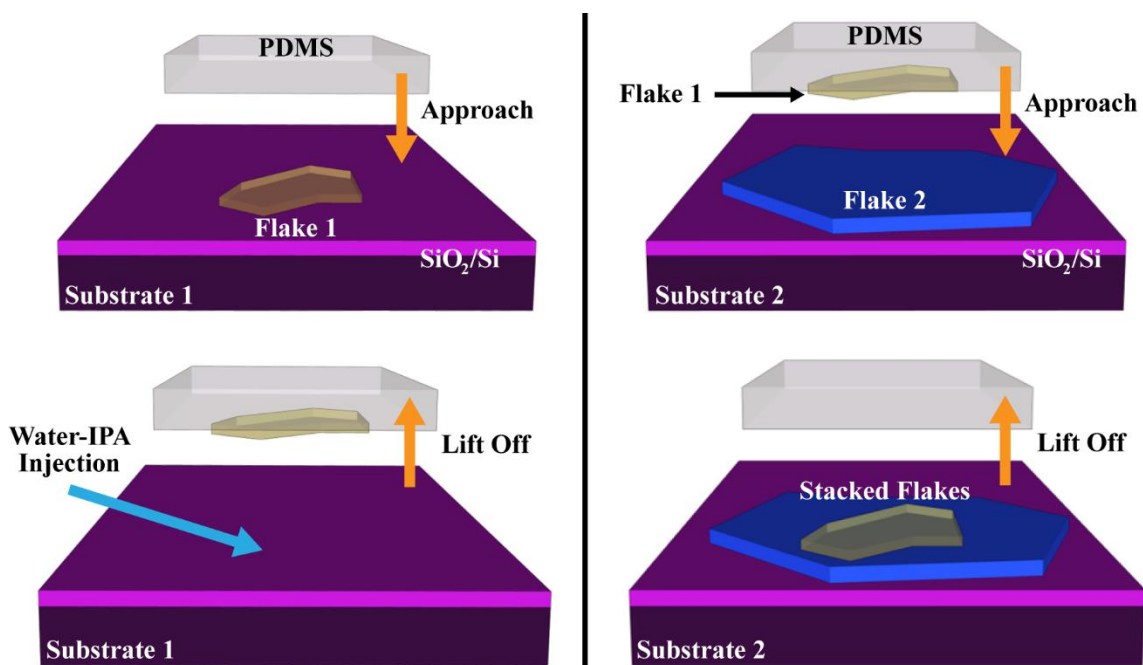


**Figure S2.** Schematic illustrating the water-assisted PDMS pick-up and transfer method of van der Waals heterostructure fabrication. Left: water-assisted transfer of a flake from a substrate surface to a PDMS stamp. Right: transfer of a flake from the stamp surface onto another surface (or flake).

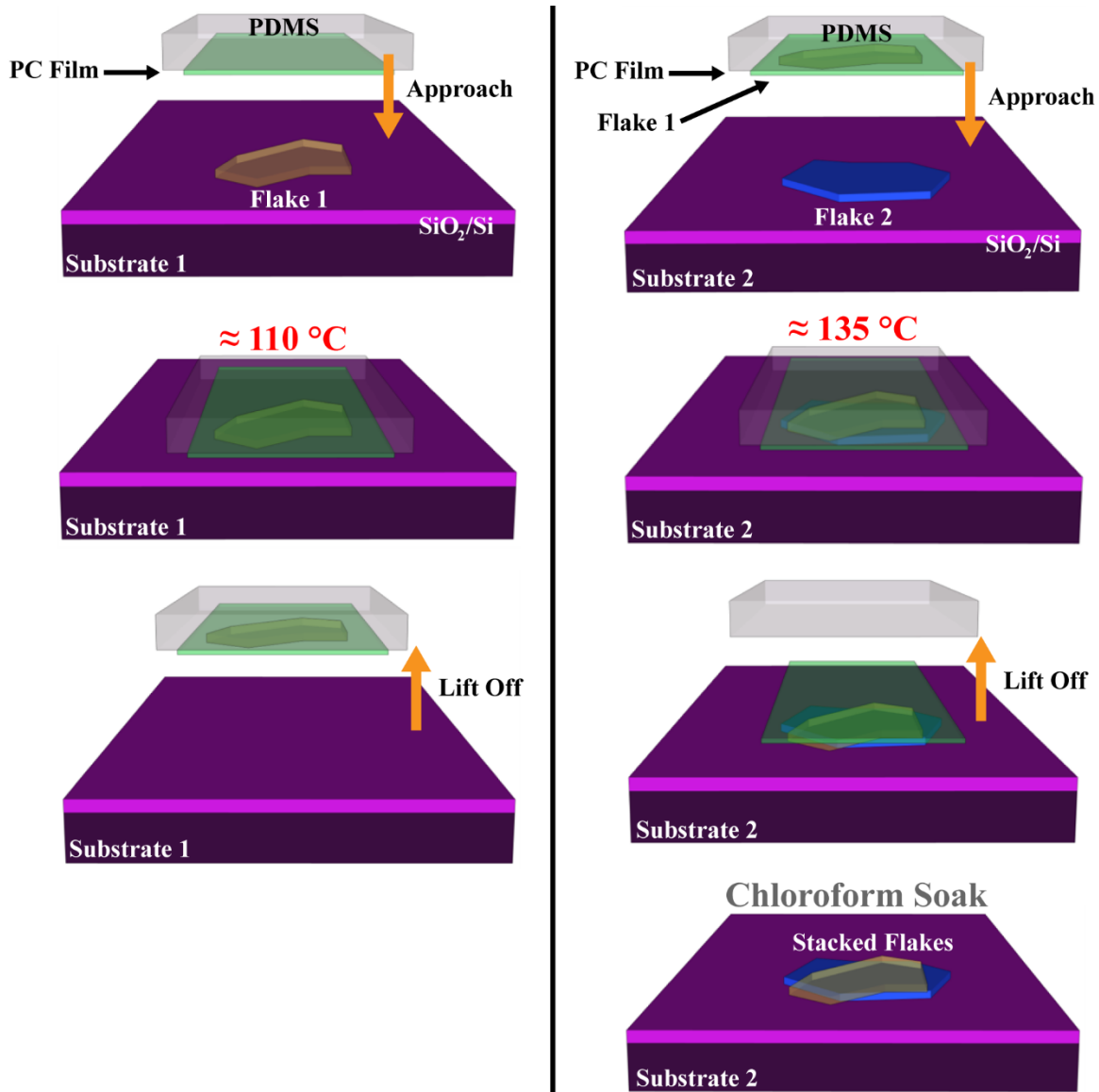


**Figure S3.** Schematic illustrating the polymer-assisted (polycarbonate, PC) dry pick-up and transfer method of van der Waals heterostructure fabrication. Left: a flake is transferred from the substrate onto a PC-coated PDMS stamp. Right: a flake is deposited from stamp onto another surface (or flake).

## Molecular Structures

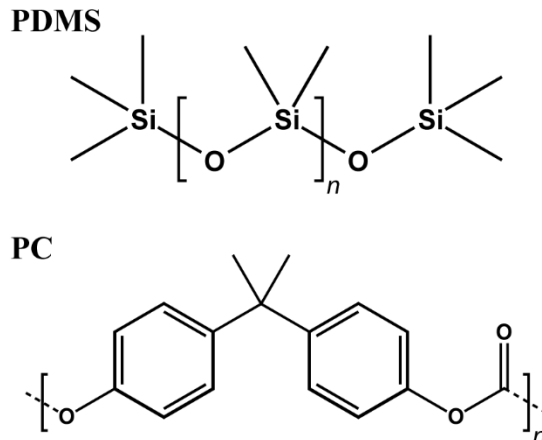


**Figure S4.** Molecular structures of polydimethylsiloxane (PDMS, top) and polycarbonate (PC, bottom). Implicit hydrogen atoms in the structures are not shown.

## Spectral Processing

A tunable quantum cascade laser (QCL) array of four chips, covering the spectral range from  $910\text{ cm}^{-1}$  to  $1900\text{ cm}^{-1}$ , was used. Absorption spectra were obtained by dividing the measured PTIR signal by the laser output intensity at each wavelength as measured by an energy meter (background spectrum). This normalization procedure can introduce spectral artifacts at the wavelengths where the laser power is very low, as typically occurs in the transition between the outputs of different QCL chips ( $1179\text{ cm}^{-1}$ ,  $1473\text{ cm}^{-1}$ , and  $1689\text{ cm}^{-1}$ ). For spectra with strong signal-to-noise ratios, these artifacts are barely noticeable but can appear as an abrupt change (step) in spectra with very low signals, such as in PTIR spectra obtained in contaminant-free regions (see, for example, spectra in Figure S8). Since such artificial steps do not correspond to real absorption features in the sample, to enable easier side-by-side comparison of PTIR spectra obtained from multiple locations on the same vdWH, the step artifacts around  $1179\text{ cm}^{-1}$  were normalized to a constant height unless otherwise noted. Additionally, for each sample the spectra were plotted with a common absorption intensity scale and displayed with a vertical offset for clarity.

## Image Processing

Topographic images were flattened by subtracting average planes fitted to the measured data and, on a line-by-line basis, vertically offset to obtain approximately matched median heights for neighboring scan lines. Widely used, open source software and custom scripts were employed to perform these processing steps, which resulted in only aesthetic improvements to the presented data and do not quantitatively impact the analysis or conclusions.

## Reference Absorption Spectra

Attenuated total reflectance Fourier transform infrared (ATR-FTIR) spectroscopy was used to obtain reference spectra of PDMS ( $\approx 250 \mu\text{m}$  thick) and PC ( $\approx 1 \mu\text{m}$  thick), as shown in Figure S5. These spectra were compared with PTIR spectra (e.g., Figures 2, 3, S6, and S7). The modest peak shifts of the ATR-FTIR spectra compared to the PTIR spectra are due to well-known effects caused by different illumination geometries.<sup>7</sup>

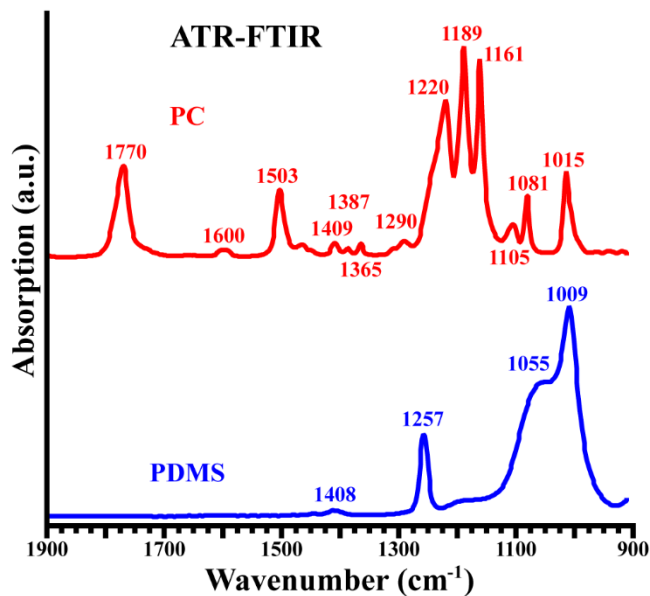


**Figure S5.** Attenuated total reflectance Fourier transform infrared (ATR-FTIR) absorption spectra of polydimethylsiloxane (PDMS, blue) and polycarbonate (PC, red).



## Additional PTIR Absorption Spectra

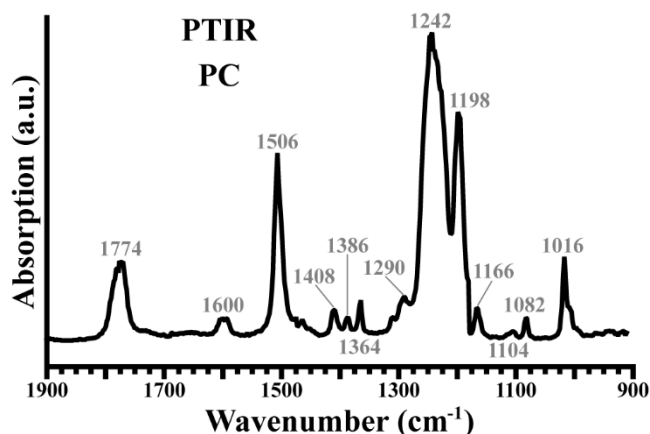


**Figure S6.** Photothermal induced resonance (PTIR) absorption spectrum measured on a thin film ( $\approx 300$  nm) of polycarbonate (PC).

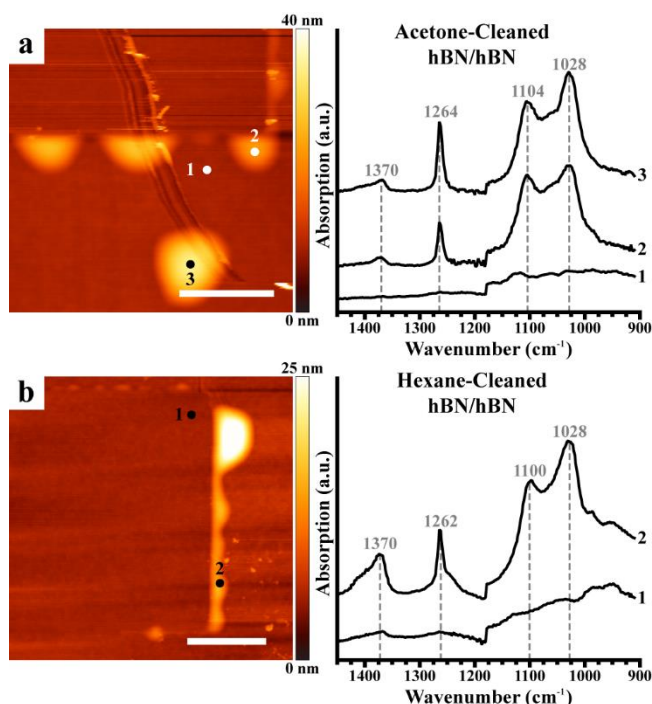


**Figure S7.** Cleaning polydimethylsiloxane (PDMS) stamps with acetone and hexane failed to reduce contaminants in van der Waals heterostructures (vdWHs). Topography (left) and photothermal induced resonance (PTIR) absorption spectra (right) obtained at the marked locations on vdWHs fabricated using the all-dry transfer method by overlaying two flakes of hexagonal boron nitride (hBN/hBN) using PDMS stamps pre-cleaned with (a) acetone and (b) hexane. Scale bars represent 2  $\mu\text{m}$ .

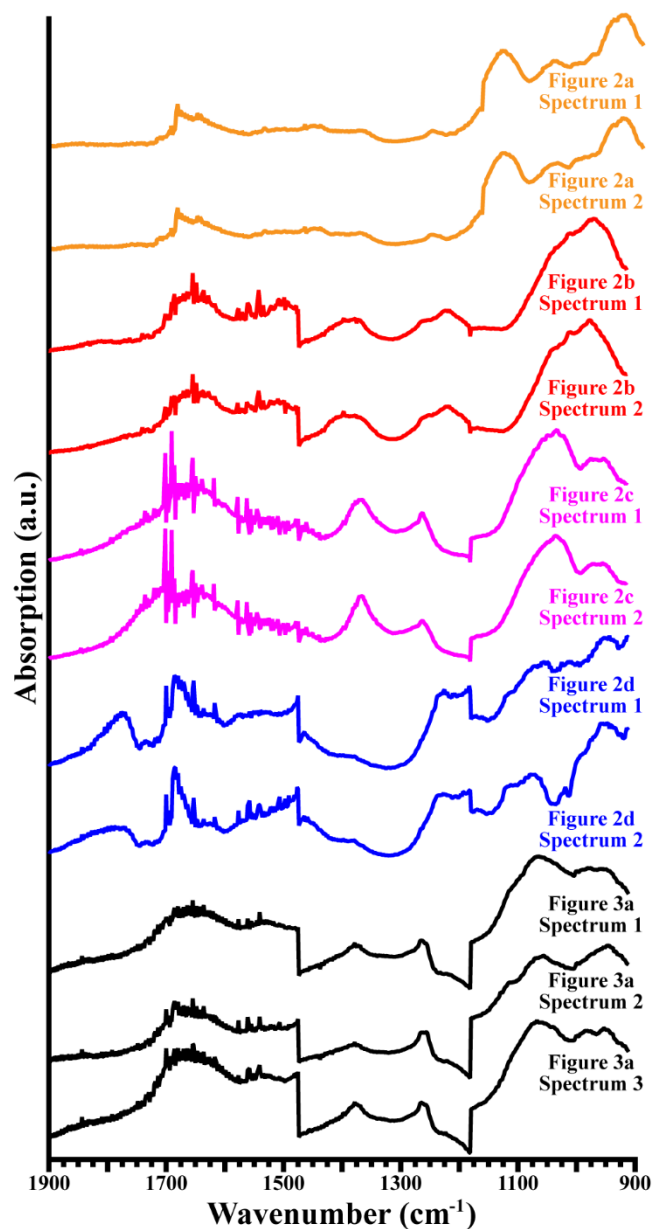


**Figure S8.** Photothermal induced resonance absorption spectra measured on nominally pristine regions of van der Waals heterostructures, away from trapped nanocontaminants. Here, spectra appear with normalized heights across their full range to emphasize their relatively weak spectral features, in contrast to their depictions in other figures, as indicated.

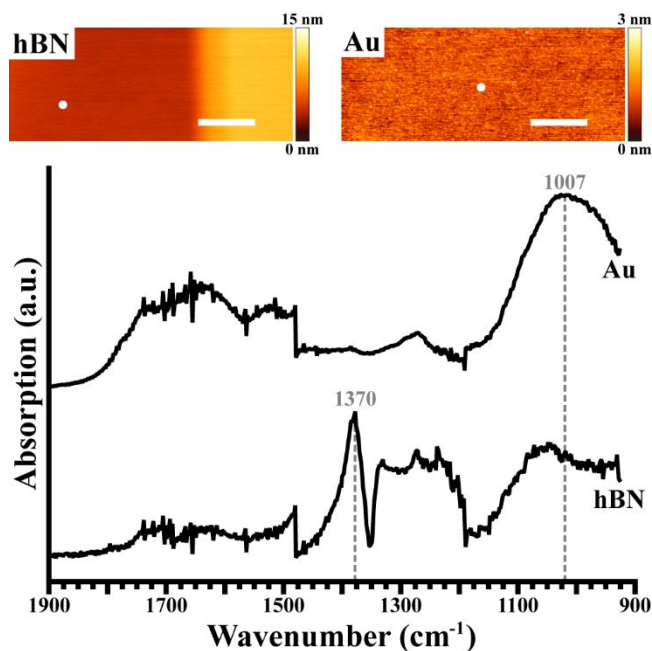


**Figure S9.** Photothermal induced resonance (PTIR) absorption spectra measured on contaminant-free surfaces. Topography (top) and PTIR spectra (bottom) obtained at the marked locations (white dots) on a flake of hexagonal boron nitride (hBN) and Au-coated SiO<sub>2</sub> surfaces. Scale bars represent 2  $\mu\text{m}$ .

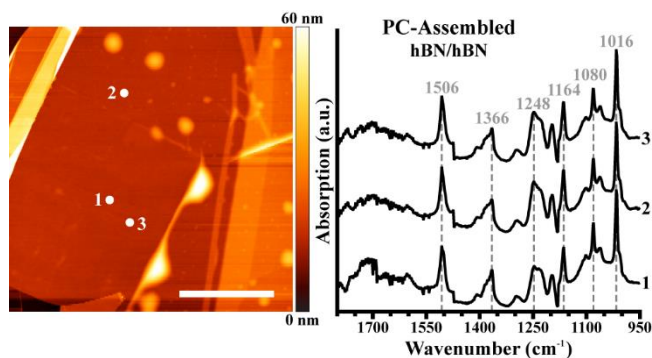


**Figure S10.** Photothermal induced resonance (PTIR) absorption spectra measured on a van der Waals heterostructure prepared using the polymer-assisted (polycarbonate, PC) dry pick-up and transfer method. Topography (left) and PTIR spectra (right) obtained at the marked locations on overlapping flakes of hexagonal boron nitride (hBN/hBN). Scale bar represents 5  $\mu\text{m}$ .

## Nanocontaminant Quantity Estimation

We estimate the approximate quantity of material probed using PTIR by modeling the contaminant bubbles as hemi-ellipsoids with volumes ( $V$ ) given by

$$V = \frac{2}{3}\pi hr^2,$$

where  $r$  represents the (assumed symmetric) lateral radius of a bubble and  $h$  represents its height. Using the dimensions estimated in Figure S11, we compute volumes of  $\approx 330$  zL and  $\approx 140$  zL for the left and right contaminant bubbles, respectively. Assuming each bubble is filled with PDMS (bulk density of  $0.965 \text{ g}\cdot\text{mL}^{-1}$  and molar volume of  $76.5 \text{ mL}\cdot\text{mol}^{-1}$ ),<sup>8</sup> these volumes correspond to  $\approx 4.3$  amol (320 zg) and  $\approx 1.8$  amol (140 zg), respectively.

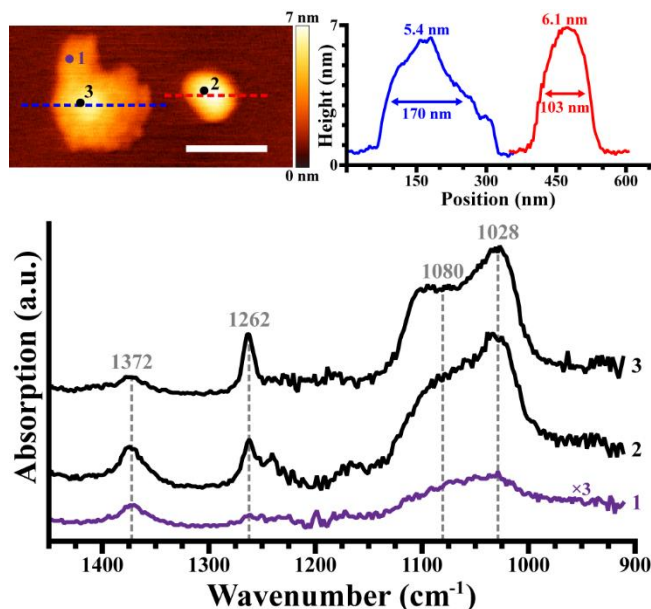


**Figure S11.** Photothermal induced resonance (PTIR) absorption spectra measured on trapped contaminants. Topography (top-left) and PTIR spectra (bottom) obtained at the marked locations on a van der Waals heterostructure made by overlaying sheets of tungsten disulfide and hexagonal boron nitride ( $\text{WS}_2/\text{hBN}$ ) using the water-assisted PDMS pick-up and transfer method. The spectrum measured at point 1 is scaled vertically by a factor of three relative to the other two spectra. Topographic line profiles (top-right) estimate the height and full width at half-maximum dimensions of each feature. Uncertainties in these measurements are assumed to be  $\pm 1$  nm (width) and  $\pm 0.1$  nm (height). The scale bar represents 200 nm.

## Supplementary References

- (1) Lee, J. N.; Park, C.; Whitesides, G. M. Solvent Compatibility of Poly(Dimethylsiloxane)-Based Microfluidic Devices. *Anal. Chem.* **2003**, *75* (23), 6544–6554. <https://doi.org/10.1021/ac0346712>.
- (2) Chuang, H.-J.; Chamlagain, B.; Koehler, M.; Perera, M. M.; Yan, J.; Mandrus, D.; Tománek, D.; Zhou, Z. Low-Resistance 2D/2D Ohmic Contacts: A Universal Approach to High-Performance WSe<sub>2</sub>, MoS<sub>2</sub>, and MoSe<sub>2</sub> Transistors. *Nano Lett.* **2016**, *16* (3), 1896–1902. <https://doi.org/10.1021/acs.nanolett.5b05066>.
- (3) Xu, M.; Liang, T.; Shi, M.; Chen, H. Graphene-Like Two-Dimensional Materials. *Chem. Rev.* **2013**, *113* (5), 3766–3798. <https://doi.org/10.1021/cr300263a>.
- (4) Hanbicki, A. T.; Chuang, H.-J.; Rosenberger, M. R.; Hellberg, C. S.; Sivaram, S. V.; McCreary, K. M.; Mazin, I. I.; Jonker, B. T. Double Indirect Interlayer Exciton in a MoSe<sub>2</sub>/WSe<sub>2</sub> van Der Waals Heterostructure. *ACS Nano* **2018**, *12* (5), 4719–4726. <https://doi.org/10.1021/acsnano.8b01369>.
- (5) Jia, H.; Yang, R.; Nguyen, A. E.; Alvillar, S. N.; Empante, T.; Bartels, L.; Feng, P. X.-L. Large-Scale Arrays of Single- and Few-Layer MoS<sub>2</sub> Nanomechanical Resonators. *Nanoscale* **2016**, *8* (20), 10677–10685. <https://doi.org/10.1039/C6NR01118G>.
- (6) Zomer, P. J.; Guimarães, M. H. D.; Brant, J. C.; Tombros, N.; van Wees, B. J. Fast Pick up Technique for High Quality Heterostructures of Bilayer Graphene and Hexagonal Boron Nitride. *Appl. Phys. Lett.* **2014**, *105* (1), 013101. <https://doi.org/10.1063/1.4886096>.
- (7) Ramer, G.; Aksyuk, V. A.; Centrone, A. Quantitative Chemical Analysis at the Nanoscale Using the Photothermal Induced Resonance Technique. *Anal. Chem.* **2017**, *89* (24), 13524–13531. <https://doi.org/10.1021/acs.analchem.7b03878>.
- (8) Chemical Retrieval on the Web. Poly(dimethylsiloxane) <https://polymerdatabase.com/polymers/Polydimethylsiloxane.html> (accessed Mar 1, 2019).